

## Article

# Genome-Wide Identification of the ABC Gene Family and Its Expression in Response to the Wood Degradation of Poplar in *Trametes gibbosa*

Jia Zhao <sup>1</sup>, Achuan Wang <sup>1,\*</sup> and Qian Wang <sup>2</sup>

<sup>1</sup> College of Computer and Control Engineering, Northeast Forestry University, Harbin 150040, China; zjwork2021@163.com

<sup>2</sup> Department of Computer Science, Durham University, Durham DH1 3LE, UK; qian.wang173@hotmail.com

\* Correspondence: wangca1964@126.com

**Abstract:** Wood-rotting fungi's degradation of wood not only facilitates the eco-friendly treatment of organic materials, decreasing environmental pollution, but also supplies crucial components for producing biomass energy, thereby reducing dependence on fossil fuels. The ABC gene family, widely distributed in wood-rotting fungi, plays a crucial role in the metabolism of lignin, cellulose, and hemicellulose. *Trametes gibbosa*, as a representative species of wood-rotting fungi, exhibits robust capabilities in wood degradation. To investigate the function of the ABC gene family in wood degradation by *T. gibbosa*, we conducted a genome-wide analysis of *T. gibbosa*'s ABC gene family. We identified a total of 12 *Tg-ABCs* classified into four subfamilies (ABCA, ABCB, ABCC, and ABCG). These subfamilies likely play significant roles in wood degradation. Scaffold localization and collinearity analysis results show that *Tg-ABCs* are dispersed on scaffolds and there is no duplication of gene sequences in the *Tg-ABCs* in the genome sequence of *T. gibbosa*. Phylogenetic and collinearity analyses of *T. gibbosa* along with four other wood-rotting fungi show that *T. gibbosa* shares a closer phylogenetic relationship with its same-genus fungus (*Trametes versicolor*), followed by *Ganoderma leucocontextum*, *Laetiporus sulphureus*, and *Phlebia centrifuga* in descending order of phylogenetic proximity. In addition, we conducted quantitative analyses of *Tg-ABCs* from *T. gibbosa* cultivated in both woody and non-woody environments for 10, 15, 20, 25, 30, and 35 days using an RT-qPCR analysis. The results reveal a significant difference in the expression levels of *Tg-ABCs* between woody and non-woody environments, suggesting an active involvement of the ABC gene family in wood degradation. During the wood degradation period of *T. gibbosa*, spanning from 10 to 35 days, the relative expression levels of most *Tg-ABCs* exhibited a trend of increasing, decreasing, and then increasing again. Additionally, at 20 and 35 days of wood degradation by *T. gibbosa*, the relative expression levels of *Tg-ABCs* peak, suggesting that at these time points, *Tg-ABCs* exert the most significant impact on the degradation of poplar wood by *T. gibbosa*. This study systematically reveals the biological characteristics of the ABC gene family in *T. gibbosa* and their response to woody environments. It establishes the foundation for a more profound comprehension of the wood-degradation mechanism of the ABC gene family and provides strong support for the development of more efficient wood-degradation strategies.

**Keywords:** ABC gene family; wood degradation; *Trametes gibbosa*; genome-wide analysis; RT-qPCR analysis



**Citation:** Zhao, J.; Wang, A.; Wang, Q. Genome-Wide Identification of the ABC Gene Family and Its Expression in Response to the Wood Degradation of Poplar in *Trametes gibbosa*. *J. Fungi* **2024**, *10*, 96. <https://doi.org/10.3390/jof10020096>

Academic Editor: Wenbing Yin

Received: 23 December 2023

Revised: 19 January 2024

Accepted: 22 January 2024

Published: 24 January 2024



**Copyright:** © 2024 by the authors. Licensee MDPI, Basel, Switzerland. This article is an open access article distributed under the terms and conditions of the Creative Commons Attribution (CC BY) license (<https://creativecommons.org/licenses/by/4.0/>).

## 1. Introduction

Poplars, known for their rapid growth, wide distribution, and short genome, among other advantages, have found extensive applications in various fields. Their fast growth makes their wood suitable for biomass energy production, and their lightweight, durable, and easy-to-process characteristics contribute to their widespread use in furniture manufacturing, construction, and the paper industry [1]. *Populus simonii* Carr × *Populus nigra* L., a hybrid

variety of poplar, inherits favorable traits from both parent species, exhibiting excellent fast-growing properties and features such as drought resistance, cold resistance, and insect resistance. As a result, it has become a key afforestation species in northern regions [2–4]. Known for its rapid growth, it typically reaches commercial timber size in a few years. Its wood generally contains a moderate amount of cellulose, making it well-suited for paper and pulp production. Therefore, it has significant potential in areas such as timber production, the paper industry, and biomass energy production [5,6].

Wood degradation is the gradual breakdown of wood into smaller compounds and organic substances in natural surroundings or specific conditions. This process plays a crucial role in the organic material cycle, contributing to the preservation of ecological balance. Furthermore, it serves as a source of raw materials for biomass energy production, offering a means to reduce reliance on fossil fuels [7–10]. However, wood, consisting of intricate compounds like lignin, cellulose, and hemicellulose, encounters numerous challenges during degradation. Lignin, the most challenging component to degrade in wood, possesses a complex structure and resists degradation by most biological enzymes due to its multiple chemical bonds. Cellulose, which is relatively more susceptible to degradation than lignin, benefits from its linear structure, facilitating enzymes in breaking  $\beta$ -1,4-glucosidic bonds. Hemicellulose presents a degradation difficulty that falls between lignin and cellulose. These components intertwine, forming a robust and less easily destructible structure, thereby heightening the complexity of wood degradation [11–13].

Wood-rotting fungi excel at degrading wood, and wood decomposition constitutes their primary way of life. They efficiently break down wood and plant residues, converting organic matter into forms more readily absorbed by other organisms. This process contributes to the natural recycling of organic materials. Furthermore, these fungi can be employed to treat waste from the wood and pulp industry, reducing environmental pollution. They present a potential for low-energy, pollution-free wood degradation and sustainable energy production [14,15]. *Trametes gibbosa*, as one of numerous wood-rotting fungi, possesses significant wood-degrading capabilities. It can release extracellular enzymes such as manganese peroxidases, lignin peroxidase, and laccase, facilitating the degradation of lignin in wood. Additionally, it produces intracellular glucanases, extracellular glucanases, and xylanases, enabling the breakdown of cellulose and hemicellulose in wood. These enzymes assist *T. gibbosa* in breaking down wood into small molecular compounds, achieving wood degradation [16–19].

The ABC gene family is widely distributed among plants, insects, and microorganisms. Genes in this family encode ABC transporters, which play a pivotal role in the metabolism of lignin, cellulose, and hemicellulose [20,21]. ABC transporters facilitate the movement of the intermediates or degradation products of lignin and cellulose between intracellular and extracellular spaces. They can create channels on the cell membrane, transporting various degradation enzymes involved in breaking down lignin and cellulose from the intracellular space to the extracellular space or other cell structures, thereby enhancing degradation efficiency. Additionally, they can expel potentially toxic substances from the cell's products into the external environment, maintaining the stability of the intracellular environment [22–24]. Researchers have conducted thorough investigations into the relationship between the ABC gene family and lignin and cellulose. For example, de Lima et al. found that the ABC gene (*Sv-ABCG17*) is a potential transporter of lignin monomers [25]. Yu et al. suggested the potential role of the ABC gene (*PgrABCG14*) in promoting plant growth and lignin accumulation [26]. Xie et al. identified ABC family genes in *Phanerochaete chryso-sporium* and suggested that the transporter protein identified in the *P. chryso-sporium* secretomes could play a role in cellobiose and/or cellodextrin uptake [27]. Based on these studies, it is speculated that the ABC gene family may have a significant impact on wood degradation. However, at present, no research has explored the specific functions of ABC family genes in wood degradation.

Here, we focused on the degradation process of *P. simonii* Carr  $\times$  *P. nigra* L. wood by *T. gibbosa*, aiming to investigate the functions and responses of the ABC gene family, conducting analyses on its structure, predicting functions, and identifying characteristics. Additionally,

we conducted a quantitative analysis of *T. gibbosa*'s ABC genes at different time points in both woody and non-woody environments using the RT-qPCR analysis, to elucidate the response of ABC gene family in the process of degrading poplar wood of *T. gibbosa*. This study establishes a solid foundation for wood-rotting fungi to contribute to the production of low-energy, environmentally friendly organic matter and sustainable energy.

## 2. Materials and Methods

### 2.1. Sample Preparation

*Trametes gibbosa* (Pers.) Fr. was provided by the Forest Pathology Laboratory of the Forestry Protection subject at the College of Forestry, Northeast Forestry University. The fungus was cultured in 250 mL conical flasks with 70 mL of LNAS medium (Low-Nitrogen Asparagine Succinic Acid) [28] and 5 mL of 15% glucose, with a pH value set at 4.5. The cultures were maintained at 27 °C under static conditions for 10, 15, 20, 25, 30, and 35 days. For the treatment group, 2 g samples of wood chips (1 × 1 × 5 cm) from *Populus simonii* Carr × *Populus nigra* L. were added to the conical flasks, while the control group had no wood chips. Each treatment condition had three biological replicate samples, and each sample was obtained by combining the mycelia from 5 flasks. After the removal of wood chips, the mycelia were collected and stored in liquid nitrogen for subsequent experimental use.

### 2.2. Identification of ABC Genes in *T. gibbosa*

Using the Pfam database "<http://pfam.xfam.org> (accessed on 5 September 2023)" [29], we conducted a search for DNA-binding domain sequences in the ABC genes of *T. gibbosa* (*Tg-ABCs*) (Table S1). Following this, the *Tg-ABCs* were classified into subfamilies using the CDD database "<https://www.ncbi.nlm.nih.gov/Structure/bwrpsb/bwrpsb.cgi> (accessed on 5 September 2023)" [30]. The DNA binding domain was subsequently visually compared using WebLogo "<http://weblogo.berkeley.edu/logo.cgi> (accessed on 6 September 2023)".

### 2.3. Phylogenetic Relationship and Motif Analyses of *Tg-ABCs* in *T. gibbosa*

The protein sequences of the *Tg-ABC* gene family were aligned using MEGA 11.0.13 software [31], and a phylogenetic tree was constructed using the neighbor-joining (NJ) method (Figure S1a). To further verify the evolutionary relationship of each protein, we constructed a phylogenetic tree of *Tg-ABC* proteins using the optimal model (LG+G+F) with the maximum likelihood (ML) method (Figure S1b). MEME "<http://meme-suite.org> (accessed on 26 September 2023)" was used to identify conserved motifs in the *Tg-ABC* protein sequences. TBtools 2.008 [32] was used to visualize the phylogenetic tree and gene structures of *Tg-ABCs*.

### 2.4. Scaffold Localization and Collinearity Analysis of *Tg-ABCs* in *T. gibbosa*

The annotation of *Tg-ABCs* was acquired from JGI databases "<https://mycocosm.jgi.doe.gov/Tragib1/Tragib1.home.html> (accessed on 28 September 2023)". *Tg-ABCs* were mapped to the genome [33] of *T. gibbosa*, and the duplication events in *Tg-ABCs* were analyzed using MCScanX in TBtools 2.008. Both of these results were visualized using TBtools 2.008.

### 2.5. Phylogenetic Relationship and Collinearity Analyses of ABC Gene Family

Segmental duplication events and collinearity between *Tg-ABCs* and homologous genes from four species of wood-rotting fungi (*T. versicolor*, *G. leucocontextum*, *L. sulphureus* and *P. centrifuga*) were analyzed using Dual Synteny Plotter. The protein sequences of these four species were obtained from the NCBI databases "<https://www.ncbi.nlm.nih.gov/protein> (accessed on 8 September 2023)". A phylogenetic tree was constructed using the neighbor-joining (NJ) method in MEGA. The results were visualized in TBtools.

## 2.6. Other Characteristic Analyses in the Tg-ABCs

ProtParam “<https://web.expasy.org/protparam> (accessed on 16 September 2023)” was used to predict the physical and chemical properties of the Tg-ABC protein (Table 1). To examine the hydrophobicity of the Tg-ABC protein, we employed ExpASy ProtScale “<https://web.expasy.org/protscale> (accessed on 16 September 2023)” (Figure S2; Table S2). TMHMM “<http://www.cbs.dtu.dk/services/TMHMM> (accessed on 16 September 2023)” was employed to forecast transmembrane helices (Figure S3; Table S3). For the prediction of phosphorylation sites, Netphos “<http://www.cbs.dtu.dk/services/NetPhos> (accessed on 16 September 2023)” was used (Figure S4; Table S4). To anticipate the topological heterogeneity model of the Tg-ABC protein, Protter “<http://wlab.ethz.ch/protter/start/> (accessed on 16 September 2023)” was employed (Figure S5; Table S5).

**Table 1.** Physicochemical properties of Tg-ABC proteins in *Trametes gibbosa*.

| ID         | Number of Amino Acids | Molecular Weight | Theoretical pI | Aliphatic Index | Grand Average of Hydropathicity | Formula  | Total Number of Atoms | Instability Index | Stability |
|------------|-----------------------|------------------|----------------|-----------------|---------------------------------|--|-----------------------|-------------------|-----------|
| gene_11539 | 1536                  | 169,596.99       | 6.28           | 107.98          | 0.186                           | C <sub>7664</sub> H <sub>12155</sub> N <sub>2041</sub> O <sub>2200</sub> S <sub>47</sub> | 24,107                | 37.98             | stable    |
| gene_11540 | 1497                  | 165,312.94       | 5.92           | 106.73          | 0.117                           | C <sub>7435</sub> H <sub>11789</sub> N <sub>1999</sub> O <sub>2176</sub> S <sub>41</sub> | 23,440                | 40.53             | unstable  |
| gene_79    | 1459                  | 161,918.99       | 7.99           | 95.42           | −0.030                          | C <sub>7256</sub> H <sub>11479</sub> N <sub>1993</sub> O <sub>2107</sub> S <sub>49</sub> | 22,884                | 35.49             | stable    |
| gene_5291  | 1476                  | 161,417.17       | 6.84           | 97.24           | 0.104                           | C <sub>7183</sub> H <sub>11477</sub> N <sub>1997</sub> O <sub>2095</sub> S <sub>65</sub> | 22,817                | 48.30             | unstable  |
| gene_2753  | 1604                  | 174,825.02       | 8.45           | 105.57          | 0.262                           | C <sub>7940</sub> H <sub>12497</sub> N <sub>2113</sub> O <sub>2241</sub> S <sub>44</sub> | 24,835                | 35.36             | stable    |
| gene_2690  | 1465                  | 164,291.53       | 6.96           | 86.22           | −0.065                          | C <sub>7446</sub> H <sub>11457</sub> N <sub>1969</sub> O <sub>2109</sub> S <sub>62</sub> | 23,043                | 39.54             | stable    |
| gene_6080  | 1463                  | 160,933.00       | 8.51           | 97.58           | −0.019                          | C <sub>7214</sub> H <sub>11504</sub> N <sub>1958</sub> O <sub>2122</sub> S <sub>41</sub> | 22,839                | 36.87             | stable    |
| gene_5257  | 1524                  | 168,164.73       | 7.00           | 86.71           | −0.018                          | C <sub>7560</sub> H <sub>11723</sub> N <sub>2059</sub> O <sub>2194</sub> S <sub>50</sub> | 23,586                | 37.30             | stable    |
| gene_5243  | 1685                  | 185,461.04       | 5.89           | 101.38          | 0.082                           | C <sub>8390</sub> H <sub>13216</sub> N <sub>2228</sub> O <sub>2432</sub> S <sub>39</sub> | 26,305                | 36.75             | stable    |
| gene_1251  | 1622                  | 178,758.07       | 5.85           | 104.06          | 0.156                           | C <sub>8094</sub> H <sub>12776</sub> N <sub>2108</sub> O <sub>2350</sub> S <sub>48</sub> | 25,376                | 39.28             | stable    |
| gene_9723  | 1594                  | 175,020.65       | 5.90           | 102.61          | 0.169                           | C <sub>7909</sub> H <sub>12477</sub> N <sub>2083</sub> O <sub>2292</sub> S <sub>50</sub> | 24,811                | 41.41             | unstable  |
| gene_8398  | 1333                  | 145,732.30       | 6.24           | 96.05           | −0.051                          | C <sub>6518</sub> H <sub>10338</sub> N <sub>1774</sub> O <sub>1951</sub> S <sub>30</sub> | 20,611                | 39.62             | stable    |

## 2.7. RT-qPCR Analysis of Tg-ABCs in Response to Wood Degradation by *T. gibbosa*

We separately extracted total RNA from *T. gibbosa* cultured under woody and non-woody environments for 10, 15, 20, 25, 30, and 35 days using the RNAPrep Pure Plant Kit (DP441) from Tiangen Biotech (Beijing) Co., Ltd., Beijing, China and selected *Gpd* as the reference gene. Real-time quantitative reverse transcription PCR (RT-qPCR) was then employed to determine the expression levels of *Tg-ABCs* and the reference gene, and the RTq-PCR was performed following the protocol of a TaKaRa one-step RT-PCR kit from Baori Medical Technology (Beijing) Co., Ltd., Beijing, China. The primer sequences are provided in Table S6. The  $2^{-\Delta\Delta C_t}$  [34] method was applied to calculate the relative expression levels of *Tg-ABCs* in woody environments compared to non-woody environments, as well as at different culture times relative to the 10-day culture.

## 3. Results

### 3.1. Identification of ABC Genes in *T. gibbosa*

We identified 12 members of the ABC gene family (*Tg-ABCs*) from the genome of *T. gibbosa*, all of which contain the conserved ABC transporter binding domain. Using WebLogo “<https://weblogo.berkeley.edu/logo.cgi> (accessed on 16 September 2023)”, we aligned the sequences of the conserved domains in the ABC transporter domains of the 12 *Tg-ABCs* (Supplementary Data S1), and the alignment results for 105 amino acids are depicted in Figure 1a. Each stack in the figure is composed of different amino acid symbols, and the overall height of the stack reflects the degree of sequence conservation at that position. The alignment results demonstrate a high conservation level of the ABC transporter domain sequences among the 12 *Tg-ABCs*. Specific amino acid positions, namely 11, 81, 82, 83, 91, and 104, exhibit complete amino acid identity, indicating excellent consistency in amino acid types at these positions.

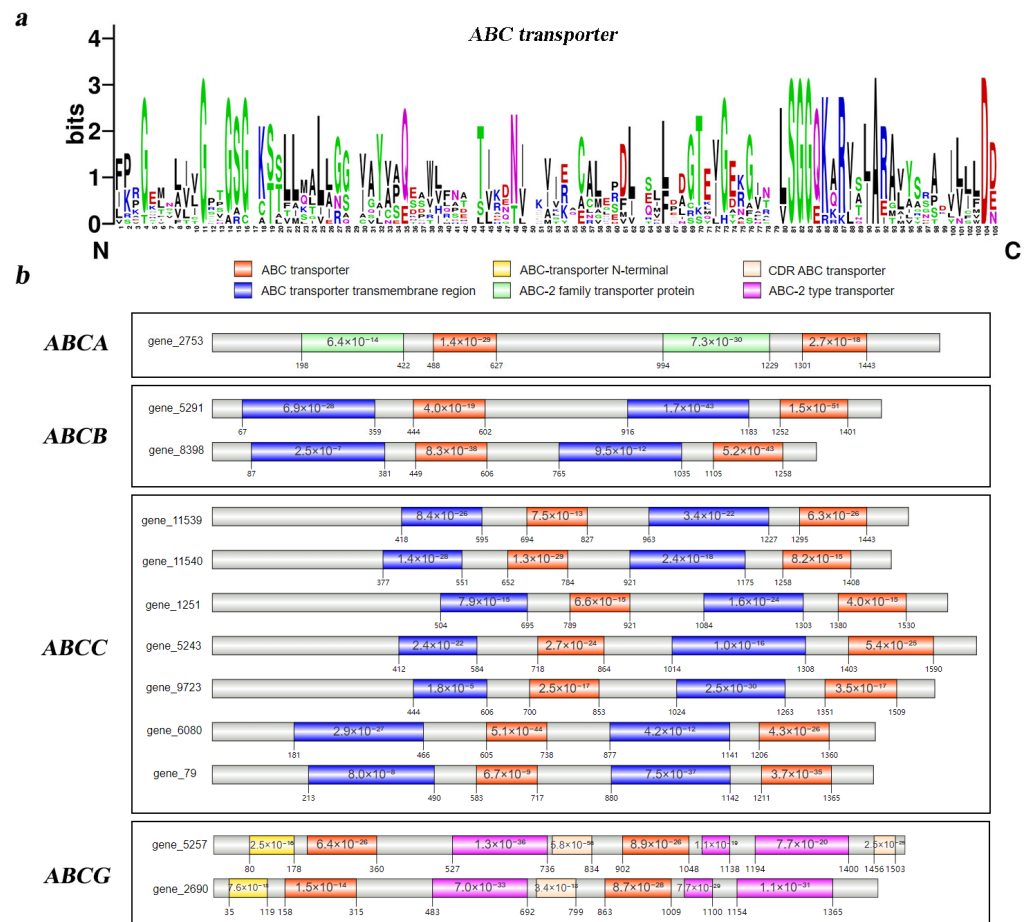


**Figure 1.** The DNA binding domain analysis of the ABC gene family in *Trametes gibbosa*. **(a)** DNA binding domain recognition marker. The symbols represent amino acids, and the height of each symbol within the stack indicates the relative frequency of that amino acid at the corresponding position; **(b)** DNA binding domain and subfamily classification of *Tg-ABCs*. Distinct domains are differentiated by different colors, with numerical values on each domain representing *p*-values. The numbers on the lower left and right sides of each domain represent the starting and ending positions of the respective domain.

The sequence alignment results for the DNA binding domain (Figure 1b) indicate that among the twelve *Tg-ABCs*, nine of them contain two conserved domains: the ABC transporter and the ABC transporter transmembrane region. Among these, seven belong to the ABCC subfamily, and two belong to the ABCB subfamily. However, in the twelve *Tg-ABCs*, three lack the ABC transporter transmembrane region. Of these genes, both *gene5257* and *gene2690* possess four conserved domains, placing them in the ABCG subfamily, while *gene2753* features an ABC-2 family transporter distinct from other *Tg-ABCs*, categorizing it as part of the ABCA subfamily.

### 3.2. Phylogenetic Relationship and Motif Analyses of *Tg-ABCs* in *T. gibbosa*

To elucidate the relationships among members of the ABC gene family in *T. gibbosa*, we constructed an NJ-phylogenetic tree using their protein sequences (Figure S1) and identified 20 motifs within the 12 *Tg-ABCs* (Figure 2).

The results indicate that genes classified within the same ABC subfamily cluster on proximate branches, sharing similar motif types. Motif 10, found in all 12 *Tg-ABCs*, is characterized as the ABC transporter-like ATP-binding domain. Genes in the ABCC subfamily exhibit a higher number of motifs ranging from 13 to 19. Genes in the ABCB

subfamily have six to seven motifs. The ABCA and ABCG subfamily genes contain the fewest motifs, with each subfamily having only two.

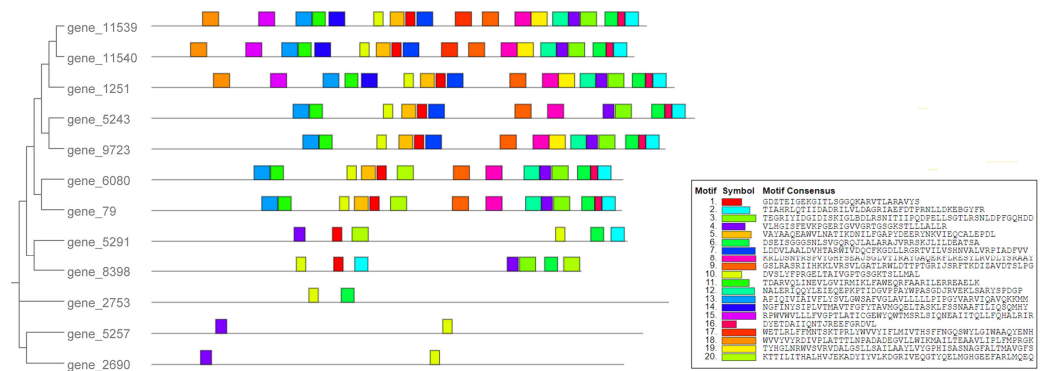


**Figure 2.** The phylogenetic tree and motifs of *Tg-ABCs* in *Trametes gibbosa*. Boxes of different colors represent different motifs.

**3.3. Scaffold Localization and Collinearity Analyses of *Tg-ABCs* in *T. gibbosa***

By analyzing the scaffold localization of the 12 *Tg-ABCs*, we discovered that only *gene5243*, *gene5257*, and *gene5291* share the same location on scaffold14, and *gene2690* and *gene2753* are found together on scaffold5, while the rest of the genes are situated on distinct scaffolds individually. This finding indicates a dispersed distribution of *Tg-ABCs* within the scaffolds of *T. gibbosa* (Figure 3a).

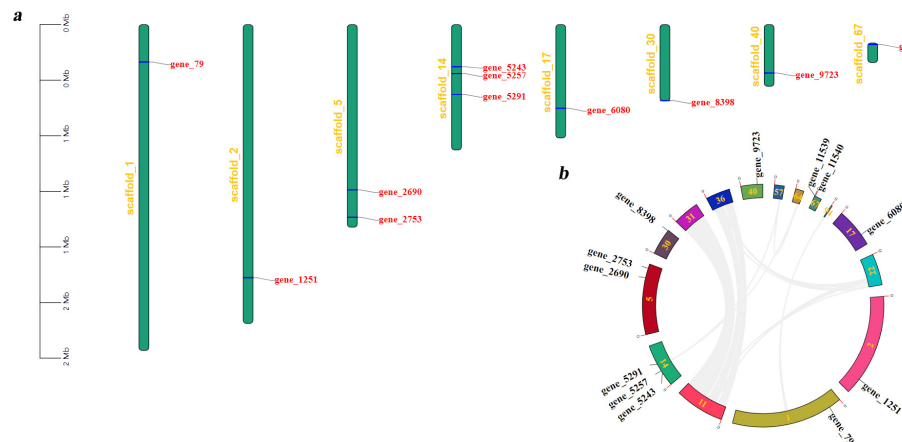


**Figure 3.** Scaffold localization and collinearity analyses of *Tg-ABCs* in *Trametes gibbosa*. (a) Distribution of *Tg-ABCs* on scaffolds; (b) segmental duplication events of *Tg-ABCs*. Displayed here are only the scaffolds that contain specific genes or collinear gene sequences.

We analyzed the segmental duplication events of *Tg-ABCs* in *T. gibbosa* and found no duplication of gene sequences. Additionally, genes located on the eight scaffolds (1, 2, 5, 14, 17, 30, 40, and 67) associated with *Tg-ABCs* displayed limited collinear gene pairs with genes on other scaffolds. In contrast, scaffolds without *Tg-ABCs*, specifically scaffold31 and scaffold36, exhibited higher numbers of collinear gene pairs with scaffold11 (Figure 3b). The integration of scaffold localization information and collinearity analysis results suggests that the functional roles of *Tg-ABCs* in *T. gibbosa* are diverse, potentially contributing differently to the process of wood degradation.

**3.4. Physicochemical Analyses of *Tg-ABCs* in *T. gibbosa***

Physicochemical analyses (Table 1) revealed that the 12 *Tg-ABC* proteins in *T. gibbosa* share comparable lengths and molecular weights. The average amino acid length is 1521.5, and the

average molecular weight is 167,619.4 Da, ranging from 145,732.30 to 185,461.04 Da. These proteins exhibit closely comparable lengths and molecular weights, displaying fluctuations around their respective averages.

Theoretical isoelectric points for Tg-ABC proteins range from 5.85 to 8.51, and the aliphatic index varies between 86.22 and 107.98. The average protein hydropathicity spans from  $-0.065$  to  $0.262$ , with the mean hydropathicity of five proteins being negative, classifying them as hydrophilic. In contrast, the remaining seven proteins exhibit positive predicted values, indicating their hydrophobic nature. These proteins are composed of five atoms, namely C, N, H, O, and S. Notably, three proteins (gene\_5291, gene\_11540, and gene\_9723) have an instability index exceeding 40, suggesting structural instability, while the majority of proteins have an index below 40, indicating stable structures.

### 3.5. Phylogenetic Relationship and Collinearity Analyses of ABC Gene Family

To elucidate the similarity between Tg-ABCs and homologous genes in other species, we selected four wood-rotting fungi (*T. versicolor*, *G. leucocontextum*, *L. sulphureus*, and *P. centrifuga*) with comparable subfamily classifications of ABC genes to *T. gibbosa*. Subsequently, we screened the protein sequences of ABC subfamilies (ABCA, ABCB, ABCC, and ABCG) from each of these fungi (Supplementary Data S2) and constructed a collinearity relationship between *T. gibbosa* and each of the other species (Figure 4).

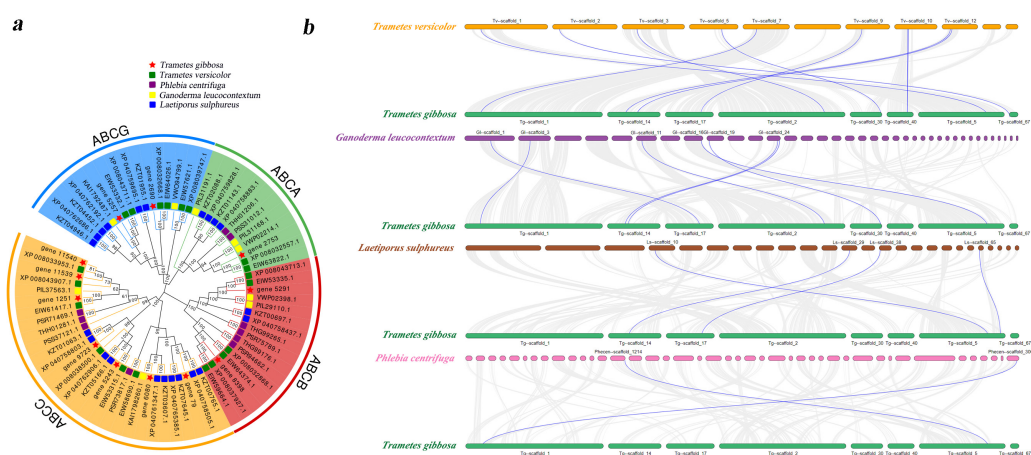


**Figure 4.** Phylogenetic tree and collinearity analyses of the ABC gene family. (a) Phylogenetic analysis of ABC proteins in *Trametes gibbosa*, *Trametes versicolor*, *Ganoderma leucocontextum*, *Laetiporus sulphureus*, and *Phlebia centrifuga*. ABC genes in *T. gibbosa* are denoted with red pentagrams, while those in the other four wood-rotting fungi are indicated with differently colored squares. Numerical values on branches represent the confidence level of each branch, with higher values indicating increased reliability; (b) collinearity relationships between genes of *T. gibbosa* and four wood-rotting fungi. The blue lines represent collinearity among ABC genes in *T. gibbosa* and other species, while the grey lines represent orthologous collinearity between the genome of *T. gibbosa* and the genomes of other species.

We conducted a phylogenetic analysis of *T. gibbosa* and four wood-rotting fungi (Figure 4a). We observed that in the phylogenetic trees of each ABC subfamily, the ABC genes of *T. gibbosa* and those of its same-genus fungus (*T. versicolor*) are positioned on relatively close branches. Additionally, the branches of ABC genes within the same subfamily are closer than those within the same species, indicating a higher degree of homology within the same ABC subfamily across different species. This suggests that ABC protein sequences exhibit a higher level of conservation during the evolutionary process.

We individually constructed collinearity relationships for *T. gibbosa* and four wood-rotting fungi (Figure 4b). In the collinearity analysis between *T. gibbosa* and its same-genus fungus (*T. versicolor*), we observed that among the twelve Tg-ABCs, nine exhibited

collinearity, with seven, four, and two *Tg-ABCs* displaying collinearity with the other three species, respectively. Integrating the results from the phylogenetic and collinearity analyses, it becomes evident that *T. gibbosa* shares a closer phylogenetic relationship with *T. versicolor*, followed by *G. leucocontextum*, *L. sulphureus*, and *P. centrifuga* in descending order of phylogenetic proximity.

### 3.6. Quantitative Analysis of *Tg-ABCs* in *T. gibbosa*

To investigate the response of *T. gibbosa*'s *Tg-ABCs* to woody and non-woody environments, we conducted a comparative analysis, examining the relative expression levels of *Tg-ABCs* at different culture times in these distinct conditions (Figure 5). The results reveal that regardless of the cultivation duration, there are significant differences in the expression levels of *Tg-ABCs* in woody and non-woody environments. Specifically, at 10 days, the majority of genes exhibited noticeable downregulation, while the upward trends of other genes were also evident, indicating the initiation of an interaction between *T. gibbosa* and wood. This suggests the involvement of *Tg-ABCs* in the wood degradation process. Between days 15, 20, and 25, there were highly significant trends of both upregulation and downregulation for all 12 *Tg-ABCs*, with peak values observed during this period. This signifies that wood degradation is most strongly influenced by *Tg-ABCs* during this timeframe. At day 30, a relatively calm period ensues, with minimal changes in the expression levels of *Tg-ABCs*, suggesting a potentially minor impact of *Tg-ABCs* on wood degradation during this stage. However, at day 35, the previous calm period is disrupted, and new fluctuations in the expression levels of *Tg-ABCs* emerge, indicating a renewed and more significant impact of *Tg-ABCs* on wood degradation at this stage.

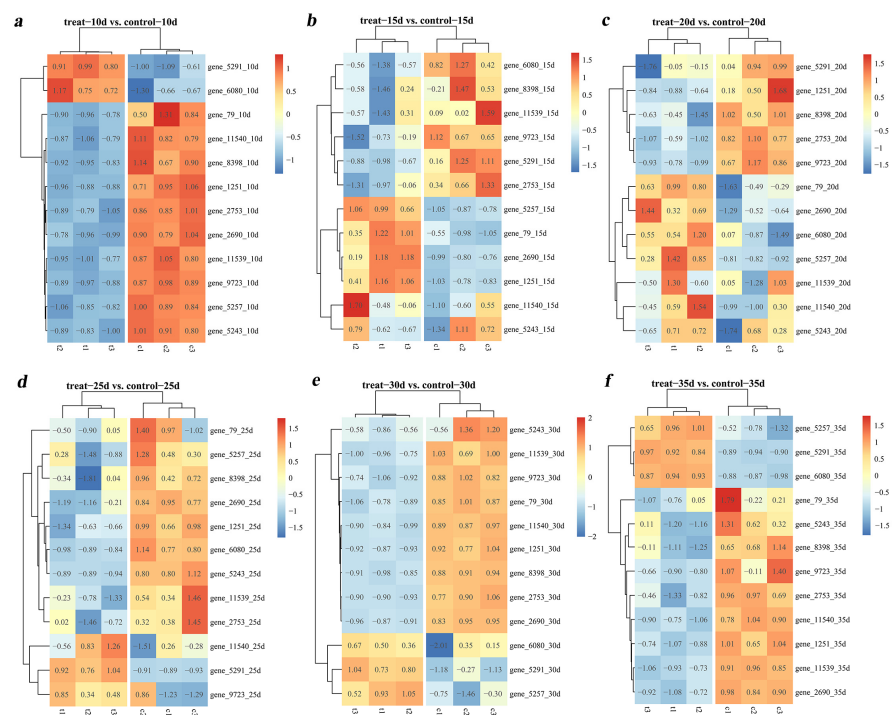


**Figure 5.** Heatmap of the relative expression levels of *Tg-ABCs* in *Trametes gibbosa* in woody and non-woody environments. The ‘treat-10d’ represents the expression levels of *Tg-ABCs* following 10 days of wood chip supplementation, while ‘control-10d’ indicates the expression level of *Tg-ABCs* without the addition of wood chips for 10 days. The series continues with ‘(a–f)’, representing the expression levels of *Tg-ABCs* at 10, 15, 20, 25, 30, and 35 days, respectively.

To further investigate the changes in the relative expression levels of *Tg-ABCs* in response to gradients of *T. gibbosa*'s wood degradation time, we analyzed the relative expression levels of *Tg-ABCs* cultivated in woody environments for 10, 15, 20, 25, 30, and



35 days (Figure 6). The results reveal that during a cultivation period of *T. gibbosa* in a woody environment lasting from 10 to 35 days, the relative expression levels of most *Tg-ABCs* followed a trend of increasing, decreasing, and increasing, with peak values observed at 20 and 35 days. At these time points, *Tg-ABCs* may have the most significant impact on *T. gibbosa*'s wood degradation. The relative expression levels of *gene11539* and *gene11540* showed a trend of increasing and then decreasing, with one fewer increase compared to most genes. *Gene8398* demonstrated a trend of increasing, decreasing, increasing, and then decreasing again, featuring one additional decrease compared to most genes. On the other hand, *gene5291* exhibited one additional increase compared to *gene8398*. As for *gene6080*, its expression had an extra decrease in the early stage compared to the majority of genes. These variations in expression trends may stem from differences in the functions of distinct genes, and different ABC subfamily genes may also play specific roles in wood degradation.

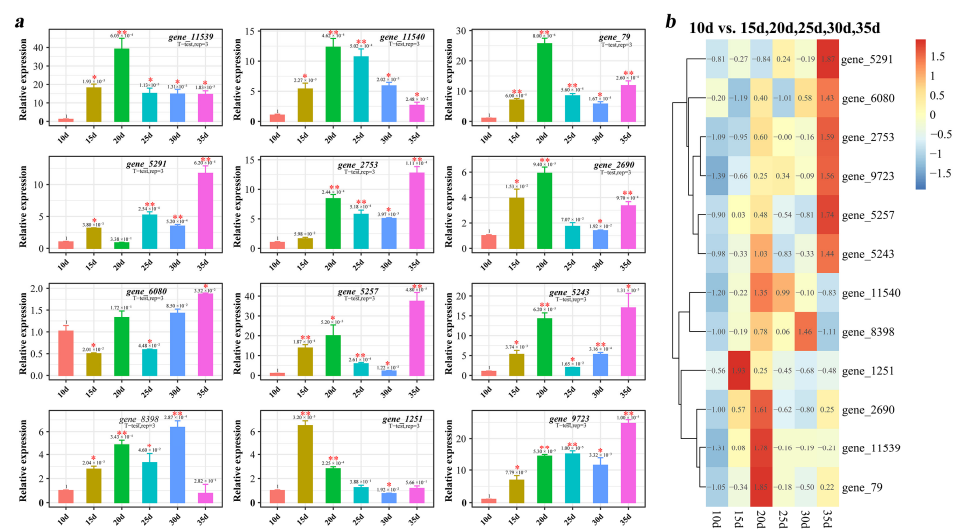


**Figure 6.** The relative expression analysis of *Tg-ABCs* in *Trametes gibbosa* under different cultivation time gradients. (a) Histogram of the relative expression analysis of *Tg-ABCs*. \*\* represents highly significant ( $p \leq 0.01$ ), \* represents significant ( $0.01 < p < 0.05$ ); (b) heatmap of the relative expression analysis of *Tg-ABCs*.

**4. Discussion**

The investigation of wood degradation holds substantial ecological and biological importance. Efficient wood degradation is vital for carbon cycling in ecosystems and provides essential technical support for sustainable biofuel production [35,36]. The ABC gene family plays a crucial role in lignin, cellulose, and hemicellulose metabolism, regulating vital substrate transport during this process [37]. *T. gibbosa*, as one of the numerous wood-rotting fungi, demonstrates efficient wood degradation capabilities [38], presenting a promising opportunity to investigate the role of the ABC gene family in wood degradation.

We identified a total of 12 *Tg-ABCs* by analyzing the genomic sequence of the ABC gene family in *T. gibbosa*. The results of the DNA binding domain alignment reveal that all of these genes contain conserved ABC transporter domains, exhibiting a high degree of sequence conservation. *Tg-ABCs* are classified into four subfamilies, ABCA, ABCB, ABCC, and ABCG. These subfamilies likely play significant roles in wood degradation, while the absence of five subfamilies [39] may have a relatively minor impact on this process. Scaffold localization results indicate that *Tg-ABCs* are dispersed on scaffolds. A collinearity analysis reveals that there is no duplication of gene sequences within the *Tg-ABCs* in the genome sequence of *T. gibbosa*. These findings collectively suggest that the functions of *T. gibbosa*'s ABC gene family in the wood degradation process may exhibit diversity. Phylogenetic and collinearity analyses of *T. gibbosa* with four other wood-rotting

fungi show that *T. gibbosa* shares a closer phylogenetic relationship with its same-genus fungus (*T. versicolor*) [40], followed by *G. leucocontextum*, *L. sulphureus*, and *P. centrifuga* in descending order of phylogenetic proximity. Additionally, the branches of ABC genes within the same subfamily are closer than those within the same species, indicating a higher degree of homology within the same ABC subfamily across different species. This suggests that ABC protein sequences exhibit a higher level of conservation during the evolutionary process, and their wood degradation characteristics may also show a higher degree of similarity [41].

To gain a deeper understanding of how *Tg-ABCs* response to wood degradation by *T. gibbosa*, we conducted quantitative analyses of the expression of *Tg-ABCs* from *T. gibbosa* cultivated in both woody and non-woody environments for 10, 15, 20, 25, 30, and 35 days using an RT-qPCR analysis. The results reveal a significant difference in the expression levels of *Tg-ABCs* between woody and non-woody environments, suggesting an active involvement of the ABC gene family in wood degradation [21,42,43]. During the wood degradation period of *T. gibbosa*, spanning from 10 to 35 days, the relative expression levels of most *Tg-ABCs* exhibited a trend of increasing, decreasing, and then increasing again. It is speculated that this trend is associated with the different products generated during various stages of wood degradation by *T. gibbosa*. In the early stages of wood degradation, *T. gibbosa* produces a significant amount of extracellular enzymes, and ABC transporters facilitate the transport of these enzymes from the extracellular space into the cell, leading to an increase in their expression levels. In the mid-phase of wood degradation, these enzymes catalyze the oxidation and decomposition of large molecules such as lignin, cellulose, and hemicellulose. At this stage, ABC transporters are not required, resulting in a decrease in their expression levels. In the later stages of wood degradation, the generation of small molecular substances like acids, alcohols, and esters prompts ABC genes to transport these substances, causing a resurgence in their expression levels [16,44,45]. The fluctuation in the relative expression levels of *Tg-ABCs* corresponds to the metabolic trajectory of wood degradation, indicating the pivotal role of *Tg-ABCs* in the process. Additionally, at 20 and 35 days of wood degradation by *T. gibbosa*, the relative expression levels of *Tg-ABCs* peak, suggesting that at these time points, *Tg-ABCs* exert the most significant impact on wood degradation by *T. gibbosa*.

## 5. Conclusions

In this study, we systematically analyzed the ABC gene family in *T. gibbosa*, examining its structure, predicting its functions, and identifying the characteristics of *Tg-ABCs*. Additionally, we also explored how *Tg-ABCs* respond to woody environments. Our findings revealed that the ABC gene family plays a crucial role in the degradation of poplar wood by *T. gibbosa*. This study lays the foundation for a deeper understanding of the wood degradation mechanism of the ABC gene family and provides strong support for the development of more efficient strategies for the biological treatment of wood and other organic materials.

**Supplementary Materials:** The following supporting information can be downloaded at <https://www.mdpi.com/article/10.3390/jof10020096/s1>, Table S1. The DNA binding domain of *Tg-ABCs*; Table S2. Hydrophobicity of *Tg-ABC* proteins; Table S3. The result of a transmembrane helical segment analysis; Table S4. Prediction of the phosphorylation site of *Tg-ABC* proteins; Table S5. The result of the topological heterogeneity model prediction; Table S6. Primer sequences for quantitative real-time PCR; Figure S1. NJ-phylogenetic and ML-phylogenetic trees; Figure S2. Hydrophobicity of *Tg-ABC* proteins; Figure S3. Transmembrane helical segments analysis; Figure S4. Phosphorylation site prediction; Figure S5. Topological heterogeneity model prediction; Supplementary Data S1. The sequences of the conserved domains in the ABC transporter domains of the 12 *Tg-ABCs*; Supplementary Data S2. The protein sequences of ABC subfamilies (ABCA, ABCB, ABCC, and ABCG) from *Trametes versicolor*, *Ganoderma leucocontextum*, *Laetiporus sulphureus*, and *Phlebia centrifuga*.

**Author Contributions:** Methodology, analysis, and writing, J.Z.; visualization, Q.W.; supervision and funding acquisition, A.W. All authors have read and agreed to the published version of the manuscript.

**Funding:** This research received no external funding.

**Data Availability Statement:** The original contributions presented in the study are included in the article/Supplementary Material, further inquiries can be directed to the first author.

**Conflicts of Interest:** The authors declare no conflicts of interest.

## References

1. Thakur, A.K.; Kumar, P.; Parmar, N.; Shandil, R.K.; Aggarwal, G.; Gaur, A.; Srivastava, D.K. Achievements and prospects of genetic engineering in poplar: A review. *New For.* **2021**, *52*, 889–920. [[CrossRef](#)]
2. Gao, S.; Li, C.; Chen, X.; Li, S.; Liang, N.; Wang, H.; Zhan, Y.; Zeng, F. Basic helix-loop-helix transcription factor *PxbHLH02* enhances drought tolerance in *Populus* (*Populus simonii* × *P. nigra*). *Tree Physiol.* **2023**, *43*, 185–202. [[CrossRef](#)] [[PubMed](#)]
3. Tao, J.; Dong, F.; Wang, Y.; Chen, H.; Tang, M. Arbuscular mycorrhizal fungi enhance photosynthesis and drought tolerance by regulating MAPK genes expressions of *Populus simonii* × *P. nigra*. *Physiol. Plant.* **2022**, *174*, e13829. [[CrossRef](#)] [[PubMed](#)]
4. Zhou, B.; Kang, Y.; Leng, J.; Xu, Q. Genome-Wide Analysis of the miRNA-mRNAs Network Involved in Cold Tolerance in *Populus simonii* × *P. nigra*. *Genes* **2019**, *10*, 430. [[CrossRef](#)] [[PubMed](#)]
5. Ahmed, A.K.M.; Fu, Z.; Ding, C.; Jiang, L.; Han, X.; Yang, A.; Ma, Y.; Zhao, X. Growth and wood properties of a 38-year-old *Populus simonii* × *P. nigra* plantation established with different densities in semi-arid areas of northeastern China. *J. For. Res.* **2020**, *31*, 497–506. [[CrossRef](#)]
6. Liu, D.; Liu, M.; Li, Z.; Wang, G.; Li, Y.; Zheng, M.; Liu, G.; Zhao, X. Variation Analysis of Growth Traits of Transgenic *Populus simonii* × *P. nigra* Clones Carrying *TaLEA* Gene. *Bull. Bot. Res.* **2015**, *35*, 540–546.
7. de Vries, L.; Guevara-Rozo, S.; Cho, M.; Liu, L.Y.; Rennecker, S.; Mansfield, S.D. Tailoring renewable materials via plant biotechnology. *Biotechnol. Biofuels* **2021**, *14*, 167. [[CrossRef](#)]
8. Vanholme, R.; De Meester, B.; Ralph, J.; Boerjan, W. Lignin biosynthesis and its integration into metabolism. *Curr. Opin. Biotechnol.* **2019**, *56*, 230–239. [[CrossRef](#)]
9. Gan, M.J.; Niu, Y.Q.; Qu, X.J.; Zhou, C.H. Lignin to value-added chemicals and advanced materials: Extraction, degradation, and functionalization. *Green Chem.* **2022**, *24*, 7705–7750. [[CrossRef](#)]
10. Zhao, L.; Zhang, J.; Zhao, D.; Jia, L.; Qin, B.; Cao, X.; Zang, L.; Lu, F.; Liu, F. Biological degradation of lignin: A critical review on progress and perspectives. *Ind. Crops Prod.* **2022**, *188*, 115715. [[CrossRef](#)]
11. Zhang, C.; Jin, Y.; Wang, F.; Shen, X.; Cheng, J.; Cai, C. Catalytic Strategies and Mechanism Analysis Orbiting the Center of Critical Intermediates in Lignin Depolymerization. *Chem. Rev.* **2023**, *123*, 4510–4601. [[CrossRef](#)]
12. Weimer, P.J. Degradation of Cellulose and Hemicellulose by Ruminant Microorganisms. *Microorganisms* **2022**, *10*, 2345. [[CrossRef](#)] [[PubMed](#)]
13. Long, L.; Hu, Y.; Sun, F.; Gao, W.; Hao, Z.; Yin, H. Advances in lytic polysaccharide monooxygenases with the cellulose-degrading auxiliary activity family 9 to facilitate cellulose degradation for biorefinery. *Int. J. Biol. Macromol.* **2022**, *219*, 68–83. [[CrossRef](#)] [[PubMed](#)]
14. Nurul-Aliyaa, Y.A.; Awang, N.A.; Mohd, M.H. Characterisation of white rot fungi from wood decayed for lignin degradation. *Lett. Appl. Microbiol.* **2023**, *76*, ovad118. [[CrossRef](#)] [[PubMed](#)]
15. Fackler, K.; Schwanninger, M. Polysaccharide degradation and lignin modification during brown rot of spruce wood: A polarised Fourier transform near infrared study. *J. Near Infrared Spectrosc.* **2010**, *18*, 403–416. [[CrossRef](#)]
16. Chen, J.; Chi, Y.; Hao, X.; Ma, L. Metabolic regulation mechanism of *Trametes gibbosa* CB1 on lignin. *Int. J. Biol. Macromol.* **2023**, *240*, 124189. [[CrossRef](#)]
17. Knezevic, A.; Stajic, M.; Milovanovic, I.; Vukojevic, J. Degradation of beech wood and wheat straw by *Trametes gibbosa*. *Wood Sci. Technol.* **2017**, *51*, 1227–1247. [[CrossRef](#)]
18. Knezevic, A.; Stajic, M.; Milovanovic, I.; Vukojevic, J. Wheat Straw Degradation by *Trametes gibbosa*: The Effect of Calcium Ions. *Waste Biomass Valorization* **2018**, *9*, 1903–1908. [[CrossRef](#)]
19. Han, M.-L.; Lin, L.; Guo, X.-X.; An, M.; Geng, Y.-J.; Xin, C.; Ma, L.-C.; Mi, Q.; Ping, A.-Q.; Yang, Q.-Y. Comparative Analysis of the Laccase Secretion Ability of Five White-rot Fungi in Submerged Fermentation with Lignocellulosic Biomass. *Bioresources* **2023**, *18*, 584–598. [[CrossRef](#)]
20. Yi, X.; Lin, L.; Mei, J.; Wang, W. Transporter proteins in *Zymomonas mobilis* contribute to the tolerance of lignocellulose-derived phenolic aldehyde inhibitors. *Bioprocess Biosyst. Eng.* **2021**, *44*, 1875–1882. [[CrossRef](#)]
21. Takeuchi, M.; Watanabe, A.; Tamura, M.; Tsutsumi, Y. The gene expression analysis of *Arabidopsis thaliana* ABC transporters by real-time PCR for screening monolignol-transporter candidates. *J. Wood Sci.* **2018**, *64*, 477–484. [[CrossRef](#)]
22. Sibout, R.; Höfte, H. Plant cell biology: The ABC of monolignol transport. *Curr. Biol.* **2012**, *22*, R533–R535. [[CrossRef](#)] [[PubMed](#)]
23. Ye, X.; Zhong, Z.; Liu, H.; Lin, L.; Guo, M.; Guo, W.; Wang, Z.; Zhang, Q.; Feng, L.; Lu, G. Whole genome and transcriptome analysis reveal adaptive strategies and pathogenesis of *Calonectria pseudoreteauidii* to *Eucalyptus*. *BMC Genom.* **2018**, *19*, 358. [[CrossRef](#)] [[PubMed](#)]
24. Yazaki, K. ABC transporters involved in the transport of plant secondary metabolites. *FEBS Lett.* **2006**, *580*, 1183–1191. [[CrossRef](#)] [[PubMed](#)]

25. de Lima, L.G.A.; Ferreira, S.S.; Simoes, M.S.; Cunha, L.X.; Fernie, A.R.; Cesarino, I. Comprehensive expression analyses of the ABCG subfamily reveal SvABCG17 as a potential transporter of lignin monomers in the model C4 grass *Setaria viridis*. *J. Plant Physiol.* **2023**, *280*, 153900. [[CrossRef](#)] [[PubMed](#)]
26. Yu, Q.; Li, J.; Qin, G.; Liu, C.; Cao, Z.; Jia, B.; Xu, Y.; Li, G.; Yang, Y.; Su, Y. Characterization of the ABC Transporter G Subfamily in Pomegranate and Function Analysis of *PgrABCG14*. *Int. J. Mol. Sci.* **2022**, *23*, 11661. [[CrossRef](#)] [[PubMed](#)]
27. Xie, C.; Gong, W.; Zhu, Z.; Zhou, Y.; Xu, C.; Yan, L.; Hu, Z.; Ai, L.; Peng, Y. Comparative secretome of white-rot fungi reveals co-regulated carbohydrate-active enzymes associated with selective ligninolysis of ramie stalks. *Microb. Biotechnol.* **2021**, *14*, 911–922. [[CrossRef](#)]
28. Kirk, T.K.; Schultz, E.; Connors, W.J.; Lorenz, L.F.; Zeikus, J.G. Influence of culture parameters on lignin metabolism by *Phanerochaete chrysosporium*. *Arch. Microbiol.* **1978**, *117*, 277–285. [[CrossRef](#)]
29. Mistry, J.; Chuguransky, S.; Williams, L.; Qureshi, M.; Salazar, G.A.; Sonnhammer, E.L.L.; Tosatto, S.C.E.; Paladin, L.; Raj, S.; Richardson, L.J. Pfam: The protein families database in 2021. *Nucleic Acids Res.* **2021**, *49*, D412–D419. [[CrossRef](#)]
30. Marchler-Bauer, A.; Derbyshire, M.K.; Gonzales, N.R.; Lu, S.; Chitsaz, F.; Geer, L.Y.; Geer, R.C.; He, J.; Gwadz, M.; Hurwitz, D.I. CDD: NCBI’s conserved domain database. *Nucleic Acids Res.* **2015**, *43*, D222–D226. [[CrossRef](#)]
31. Tamura, K.; Stecher, G.; Kumar, S. MEGA11: Molecular Evolutionary Genetics Analysis Version 11. *Mol. Biol. Evol.* **2021**, *38*, 3022–3027. [[CrossRef](#)] [[PubMed](#)]
32. Chen, C.; Wu, Y.; Li, J.; Wang, X.; Zeng, Z.; Xu, J.; Liu, Y.; Feng, J.; Chen, H.; He, Y. TBtools-II: A “One for All, All for One” Bioinformatics Platform for Biological Big-data Mining. *Mol. Plant* **2023**, *16*, 1733–1742. [[CrossRef](#)] [[PubMed](#)]
33. Hage, H.; Miyauchi, S.; Viragh, M.; Drula, E.; Min, B.; Chaduli, D.; Navarro, D.; Favel, A.; Norest, M.; Lesage-Meessen, L. Gene family expansions and transcriptome signatures uncover fungal adaptations to wood decay. *Environ. Microbiol.* **2021**, *23*, 5716–5732. [[CrossRef](#)] [[PubMed](#)]
34. Livak, K.J.; Schmittgen, T.D. Analysis of relative gene expression data using real-time quantitative PCR and the 2<sup>(-Delta Delta C(T))</sup> Method. *Methods* **2001**, *25*, 402–408. [[CrossRef](#)] [[PubMed](#)]
35. Khan, M.U.; Ahring, B.K. Lignin degradation under anaerobic digestion: Influence of lignin modifications—A review. *Biomass Bioenergy* **2019**, *128*, 105325. [[CrossRef](#)]
36. Jiang, B.; Jiao, H.; Guo, X.; Chen, G.; Guo, J.; Wu, W.; Jin, Y.; Cao, G.; Liang, Z. Lignin-Based Materials for Additive Manufacturing: Chemistry, Processing, Structures, Properties, and Applications. *Adv. Sci.* **2023**, *10*, 2206055. [[CrossRef](#)] [[PubMed](#)]
37. Tang, T.; Kong, W.; Ren, K.; Cheng, H. Advance of Research in Function of Plant ABC Transporters. *Acat Agric. Boreali-Occident. Sin.* **2023**, *32*, 1–10.
38. Chi, Y.; Gu, X. Advances in the Research of *Lenzites gibbosa* (Pers.) Hemmi. *J. Jilin Agric. Univ.* **2021**, *43*, 275–282.
39. Viglas, J.; Olejnikova, P. An update on ABC transporters of filamentous fungi—from physiological substrates to xenobiotics. *Microbiol. Res.* **2021**, *246*, 126684. [[CrossRef](#)]
40. Chi, Y.; Yan, H.; Wu, S. Phylogenetic Analysis and Cloning of the Gene *Lg-mnp2* and *Lg-mnp3* of *Lenzites gibbosa* CB1. *J. North-East For. Univ.* **2019**, *47*, 64–87.
41. Kovalchuk, A.; Driessen, A.J.M. Phylogenetic analysis of fungal ABC transporters. *BMC Genom.* **2010**, *11*, 177. [[CrossRef](#)] [[PubMed](#)]
42. Kaneda, M.; Schuetz, M.; Lin, B.S.P.; Chanis, C.; Hamberger, B.; Western, T.L.; Ehrling, J.; Samuels, A.L. ABC transporters coordinately expressed during lignification of *Arabidopsis* stems include a set of ABCBs associated with auxin transport. *J. Exp. Bot.* **2011**, *62*, 2063–2077. [[CrossRef](#)] [[PubMed](#)]
43. Michalska, K.; Chang, C.; Mack, J.C.; Zerbs, S.; Joachimiak, A.; Collart, F.R. Characterization of Transport Proteins for Aromatic Compounds Derived from Lignin: Benzoate Derivative Binding Proteins. *J. Mol. Biol.* **2012**, *423*, 555–575. [[CrossRef](#)] [[PubMed](#)]
44. Dao, A.T.N.; Loenen, S.J.; Swart, K.; Dang, H.T.C.; Brouwer, A.; de Boer, T.E. Characterization of 2,3,7,8-tetrachlorodibenzo-p-dioxin biodegradation by extracellular lignin-modifying enzymes from ligninolytic fungus. *Chemosphere* **2021**, *263*, 128280. [[CrossRef](#)]
45. Leriche-Grandchamp, M.; Flourat, A.; Shen, H.; Picard, F.; Giordana, H.; Allais, F.; Fayeulle, A. Inhibition of Phenolics Uptake by Ligninolytic Fungal Cells and Its Potential as a Tool for the Production of Lignin-Derived Aromatic Building Blocks. *J. Fungi* **2020**, *6*, 362. [[CrossRef](#)]

**Disclaimer/Publisher’s Note:** The statements, opinions and data contained in all publications are solely those of the individual author(s) and contributor(s) and not of MDPI and/or the editor(s). MDPI and/or the editor(s) disclaim responsibility for any injury to people or property resulting from any ideas, methods, instructions or products referred to in the content.